Eur. Phys. J. C (2024) 84:730
https://doi.org/10.1140/epjc/s10052-024-13120-x

THE EUROPEAN PHYSICAL JOURNAL C

Regular Article - Theoretical Physics

The role of pressure anisotropy on quark stars in gravity's rainbow

Ayan Banerjee[1,a], **Anirudh Pradhan**[2,b], **B. Dayanandan**[3,c], **Akram Ali**[4,d]

[1] Atrophysics Research Centre, School of Mathematics, Statistics and Computer Science, University of KwaZulu-Natal, Private Bag X54001, 4000 Durban, South Africa
[2] Centre for Cosmology, Astrophysics and Space Science, GLA University, Mathura, Uttar Pradesh 281 406, India
[3] Natural and Medical Sciences Research Centre, University of Nizwa, 616 Nizwa, Sultanate of Oman
[4] Department of Mathematics, College of Science, King Khalid University, 9004 Abha, Saudi Arabia

Received: 6 June 2024 / Accepted: 14 July 2024

Abstract This work is seeking for the existence of stable quark stars (QSs) in the framework of a modified theory of gravity known as gravity's rainbow. This modification comes from the fact that the geometry of spacetime depends on the energy of the test particle. We solve numerically the modified TOV equations and present the mass–radius (M–R) diagram for quark matter equations of state. To constrain the allowed values of the model parameters, we use current astrophysical measurements of the masses and radii of neutron stars. Finally, we investigate the dynamical stability of the hydrostatic equilibrium equations in gravity's rainbow by analyzing the static stability, adiabatic index, and sound velocity profiles.

1 Introduction

During the past few decades, there have been drastic improvements in astronomical observations that have opened a new window to look at high-energy phenomena on relatively small astronomical scales. This observation raised an intriguing question related to the properties of matter at high densities and temperatures in neutron stars (NSs). Under such extreme conditions, it's hard to deal with the matter in a laboratory; therefore, the equation of state (EoS) of dense matter (expected to be many times higher than the nuclear saturation density) cannot be determined by experimental methods alone [1,2]. Indeed, substantial efforts have been devoted to addressing this situation while determining the gross structure of compact stars. Within these constraints, scientists proposed a variety of exotic states of matter, such as Bose-Einstein, quark-gluon plasma, high-temperature superconductors, and so on.

More realistically, strong coupling-based phenomena offer an exciting arena in particle physics and lead to the discovery of of new principles. The outcome mainly depends on the interaction between quarks and gluons, as described by quantum chromodynamics (QCD) [3]. As a result, QCD provides a successful description of matter at extreme environments, such as the astrophysics of compact stars [4–6]. in non-central, high-energy heavy ion collisions [7–9] and in the early universe [10,11]. It is therefore speculated that such a phase transitions of hadronic matter to deconfined quark matter could be occur inside the cores of massive NSs. In particular, most of the examined model favor a first-order deconfining transition [12,13].

Even more intriguing, the predicted quark matter in a core of NS was first proposed by Itoh [14] in 1970. Prior to that, Ivanenko and Kurdgelaidze [15] thought that a quark star (QS) might exist in 1965. The key ingredient to describe a QS is quark matter (strange quark matter), characterized most simply by *up, down and strange* quarks (together with an appropriate number of electrons to guarantee electrical neutrality) satisfying the Bodmer–Witten hypothesis [16,17]. According to this conjecture, quark matter may actually be more stable than ordinary nuclear matter (see [18] for a review).

In this paper, we investigate the possible existence of QS in the context of rainbow gravity. For quark matter, we Consider the MIT bag model. Specifically, the MIT bag model, developed at the Massachusetts Institute of Technology in Cambridge (USA) in 1974, considered as a successful phenomenological model for quark confinement. Using this model, authors in [19] have obtained $2M_{\odot}$ hybrid stars for reasonable values of the bag model parameters; see also Ref.

[a] e-mail: ayanbanerjeemath@gmail.com (corresponding author)
[b] e-mail: pradhan.anirudh@gmail.com
[c] e-mail: baiju@unizwa.edu.om
[d] e-mail: akali@kku.edu.sa

Published online: 23 July 2024

[20]. In particular, it was found that the MIT bag model can successfully describe the structural properties of SQSs in a modified theory of gravity; see, e.g., [21–28]. Moreover, QSs with the inclusion of charged effect have also been found in modified gravity theory [29–33].

The goal of the present article is to see the effect of anisotropic pressure and investigate the structural properties of QSs in a modified theory of gravity known as rainbow gravity. The theory of rainbow gravity has been proposed as a generalization of doubly (or deformed) special relativity. In this formalism, the geometry of spacetime depends on the energy of the probe particle, which affects the spacetime background and leads to distinct distortions in spacetime. Within the framework of rainbow gravity, exact black hole solutions and their interesting properties have been studied by many authors in [34–38]. Most recently, gravastar and wormhole solutions have been found in gravity's rainbow theory; see Refs. [39,40]. Such modification of gravity can address a number of important physical properties of astronomical objects at extreme situation, such as dark stars [41] and neutorn stars [42]. Considering the same modified gravity, our interest lies in analyzing the structural properties of QSs. Later, we consider available mass and radius measurements of pulsars to constrain the free model parameters.

The work is structured as follows. In Sect. 2, we briefly recall the basic equations of rainbow gravity. Assuming spherically symmetric metric, we obtain the modified Tolman–Oppenheimer–Volkoff (TOV) equations that describe solutions of stellar structure. In Sect. 3 we present an overview of the equations of states (EoSs) that have been used for the quark star model. Section 4 is devoted to studying our numerical results focusing, in particular, on the mass–radius relation. We then examine the dynamical stability of the stellar configuration under consideration in Sect. 5. Finally, in Sect. 6 we summarize the results and draw conclusions.

2 Review of Gravity's Rainbow and stellar structure equations

2.1 Rainbow theory

The theory of doubly special relativity (DSR) has been proposed by Amelino-Camelia [43] as a generalization of special relativity, see also Ref. [44] for more. Here, the terminology "doubly special" is a very suggestive term as DSR possess two quantities that are observer independent, the speed of light and the Planck energy. Despite the success of DSR there are several doubts that has so far no satisfactory answer, such as the so-called "soccer ball" problem. To overcome this problem, Magueijo and Smolin [45] proposed a generalization of the DSR to the curved spacetimes. Such theory is called as rainbow gravity (or gravity's rainbow) assuming the geometry of spacetime depends on the energy of the test particle. Under these conditions varying particle energies lead to distinct distortions in spacetime, and modify the standard relativistic dispersion relation in the high-energy regime (or Planck scale). Thereby, the associated modification could be written as:

$$E^2\Xi(x)^2 - p^2\Sigma(x)^2 = m^2. \tag{1}$$

where $\Xi(x)$ and $\Sigma(x)$ are known to be rainbow functions that are characterized by the dimensionless ratio $x = E/E_p$. Here, E is the relativistic total energy of the probe particle and E_p is the Planck energy, represented as $E_p = \sqrt{\frac{\hbar c^5}{G}}$. Since, the rainbow functions with specific functional forms are responsible for this modification in the ultraviolet regime and plays a significant role within the framework of Rainbow gravity. However, in the low energy scale where $x = E/E_p \to 0$, the rainbow functions satisfy the following relations

$$\lim_{x\to 0}\Xi(x) = 1, \quad \lim_{x\to 0}\Sigma(x) = 1, \tag{2}$$

and the standard energy dispersion relation is recovered. For this purpose, authors in [45] had pointed out that metrics are given in terms of energy-dependent, which is

$$g^{\mu\nu}(x) = \eta^{ab}e^{\mu}_{a}(x)\otimes e^{\nu}_{b}(x), \tag{3}$$

where the energy-dependent vierbein fields represented as $e^{\mu}_{a}(x)$ with the relation

$$e^{\mu}_{0}(x) = \frac{1}{\Xi(x)}\tilde{e}^{\mu}_{0}, \quad e^{\mu}_{k}(x) = \frac{1}{\Sigma(x)}\tilde{e}^{\mu}_{k}, \tag{4}$$

and the tilde quantities refer to the energy-independent tetrads, where the index k is used to denote the spatial coordinates and assume the values (1, 2, 3). It may be noted that the modified form of the relativistic dispersion relation by the rainbow functions is not unique, because they are implicitly dynamical functions of the coordinates. Thus, the gravity's rainbow is a promising candidate to probe quantum gravitational effects in the core of a compact star. In this prescription, the equation of motion in gravity's rainbow turns out to be [45]

$$G_{\mu\nu}(x) \equiv R_{\mu\nu}(x) - \frac{1}{2}g_{\mu\nu}(x)R(x) = k(x)T_{\mu\nu}(x), \tag{5}$$

where $G_{\mu\nu}(x)$ is the Einstein tensor with $k(x) = 8\pi G(x)$, and the stress-energy tensor is given by $T_{\mu\nu}(x)$ which acts as the source of spacetime curvature. For simplicity, we work in units where $G(x) = 1$.

2.2 Modified TOV equations of gravity's rainbow

Following the approach presented in Ref. [45], one can replace the conventional spherical symmetric metric by a rainbow metric in the following form,

$$ds^2 = -\frac{e^{2\Phi(r)}}{\Xi^2(x)}dt^2 + \frac{e^{2\lambda(r)}}{\Sigma^2(x)}dr^2 + \frac{r^2}{\Sigma^2(x)}d\Omega^2, \tag{6}$$

where $\Phi(r)$ and $\lambda(r)$ are radial dependent functions and we have defined $d\Omega^2 = (d\theta^2 + \sin\theta^2 d\phi^2)$. Also, the rainbow functions $\Xi(x)$ and $\Sigma(x)$ do not depend on spacetime coordinates (r, t, θ, ϕ).

In this work, we aim to explore the effect of local anisotropy within a QS. For such a fluid, the stress-energy tensor of the form [63]

$$T_{\mu\nu} = (\rho + p_t)u_\mu u_\nu + p_t g_{\mu\nu} - (p_t - p_r)\chi_\mu\chi_\nu, \tag{7}$$

where $\rho(r)$ is the energy density with $p_r(r)$ and $p_t(r)$ are the radial and transverse pressure, respectively. The fluid 4-velocity is define as

$$u^\mu = \left(\frac{\Xi(x)}{e^{\Phi(r)}}, 0, 0, 0\right), \tag{8}$$

with following restriction $u_\mu u^\mu = -1$ and χ_μ is the unit normal vector in the radial direction with $\chi_\mu\chi^\mu = 1$.

Finally, using the above mentioned metric (6) and stress-energy tensor (7), we are in a position to write down the modified Tolman–Oppenheimer–Volkoff (TOV) equations for a spherically symmetric and static metric [42]

$$M_{\rm eff}(r, x) = \int_0^r \frac{4\pi r^2\rho(r)}{\Sigma^2(x)}dr \equiv \frac{m(r)}{\Sigma^2(x)}, \tag{9}$$

$$p_r' = -(\rho + p_r)\Phi' + \frac{2}{r}(p_t - p_r), \tag{10}$$

$$\Phi'(r) = \frac{M_{\rm eff}(r, x)\Sigma^2(x) + 4\pi r^3 p_r(r)}{r\,(r - 2M_{\rm eff}(r, x))\,\Sigma^2(x)}, \tag{11}$$

where prime denotes the first order derivative with respect to the radial coordinate, r. The gravitational field equations (9)–(11) describing a stellar structure in rainbow gravity should be closed by assuming a constitutive equation of state (EoS) relating the pressures and the density. Furthermore, Eqs. (9)–(11) with an *ad hoc* EoS (which we will discuss later) can be solved numerically by imposing a suitable boundary conditions $m(0) = 0$ and $\rho(0) = \rho_c$, and then integrates outward to a radius $r = R$ where radial pressure vanishes at the surface of the star i.e., $p_r(R) = 0$ for selecting ρ_c.

3 Theoretical framework

3.1 MIT bag model

Theoretically, QSs are composed of entirely or almost entirely of quark matter which could be the true ground state of baryonic matter with an energy per baryon $\epsilon \equiv E/A$ could be less than that of the most stable atomic nucleus, such as ^{56}Fe and ^{62}Ni. On the other hand, the landmark detection of GWs by the Advanced LIGO and Advanced Virgo detectors [46–48] has opened up the prospect of testing the internal structure of ultra-massive NSs. Beside that it helps us to choose reliably EoS, give also insight on the behavior of matter at such high densities. In this sense, it is speculated that deconfined quark matter exists in the core of massive NSs. As a result, the EoS of quark matter can have a significant role in pushing up massive NSs detected in the last decade or so.

Here we focus on the most successful phenomenological model for quark matter is the MIT bag model to explain hadrons in terms of quarks [49]. According to this model, quarks are asymptotically free and confined in a finite region called 'bag'. Therefore, MIT bag model can be viewed as a relativistic particle confined in a box. The EoS relating energy density and pressure is given by:

$$p_r = \frac{1}{3}(\rho - 4B). \tag{12}$$

where B represents the bag constant with vanishing external pressure at $\rho = 4B$. The parameter value of B typically lies within a range of $57 \leq B \leq 92$ MeV/fm ^{3}, as can be seen in Refs. [50,51]. Throughout our numerical calculation, we choose the value for $B = 60$ MeV/fm^3, and using this value one can predict the existence of massive compact object satisfying $2M_\odot$ limit within general relativity (GR) context (see Refs. [52–54] for a detailed review).

Meanwhile, we consider the quasilocal EoS [55] that describe local anisotropy pressure inside a compact star. Within this approach, various anisotropic solutions were found in both GR and modified gravity theory. So the pressure anisotropy, in our case leads to the following expression

$$\Delta \equiv p_\perp - p_r = \beta p_r \mu. \tag{13}$$

Here β is a dimensionless free parameter that measures the deviation from isotropy in the fluid. Since, the values of β lies within the range $-2 \leq \beta \leq 2$ provides a good accuracy with the data obtained from observational astronomy (check, e.g., [56–63] and their references). Further, $\mu \equiv 2m(r)/r$ represents the measure of local compactness and $m(r)$ is the gravitational mass enclosed within a radius r. Since the effect of anisotropy vanishes at the center of the star i.e., $\Delta = 0$ when $r \to 0$, and thereby recovering the isotropic solution. This anisotropy model also permits the vanishing pressure

Table 1 The table summarizes results for QS properties, such as the maximum mass $M_{\max}$ and their corresponding radius $R_{\max}$ in units of $M_\odot$ and km, respectively. The range for parameters are $B = 60$ MeV/fm^3 and $\beta = 0.5$ with varying $\Sigma(x) \in [0.85, 1.15]$

$\Sigma(x)$	M $[M_\odot]$	R_M [km]	ρ_c [MeV/fm^3]	M/R
0.85	1.80	9.30	1069	0.3
0.90	1.91	9.84	1069	0.3
1.00	2.13	10.94	1069	0.3
1.05	2.23	11.48	1069	0.3
1.10	2.39	12.03	1069	0.3
1.15	2.45	12.57	1069	0.3

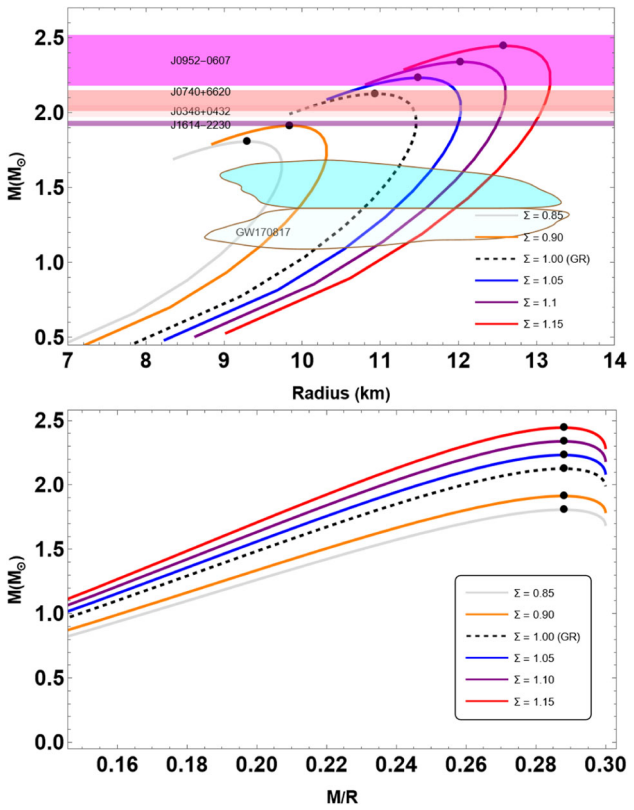

Fig. 1 Mass–radius and maximum compactness diagrams of QSs in rainbow gravity. For our analysis, we adopt the $B = 60$ MeV/fm^3 and $\beta = 0.5$ with varying $\Sigma(x) \in [0.85, 1.15]$. The boundaries of each color band are obtained form the mass–radius measurement of the maximum-mass of pulsars: PSR J0348+0432 (LightRed) [64], PSR J0740+6620 (Pink) [65] and PSR J0952-0607 (Magenta) [66], PSR J1614-2230 [67] (Purple). The shaded areas correspond to the constraints from the binary NS merger GW170817 event [68]. The case $\Sigma(x) = 0$ (dashed-black line), gives the curve for GR solution

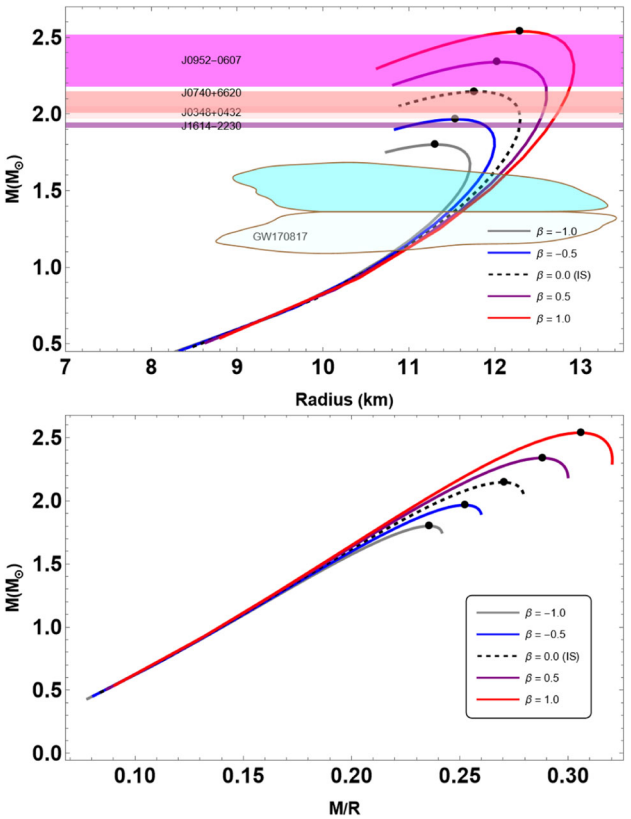

Fig. 2 Mass–radius and maximum compactness diagrams of QSs in rainbow gravity. For our analysis, we adopt the $B = 60$ MeV/fm^3 and $\Sigma(x) = 1.1$ with varying $\beta = \in [-1.0, 1.0]$. The case $\beta = 0$ (dashed-black line), gives the curve for isotropic solution. To compare with observational constraints, we indicate the same pulsar measurements as in Fig. 1

components at the surface of the star, i.e., $p_r\,(r \to R) = p_\perp\,(r \to R) = 0$. Moreover, the expression (13) vanishes at $\beta = 0$ which satisfy the regularity conditions at stellar interior. In our calculation we use the range $\beta \in [-1, 1]$, where the changes in mass–radius relation are visible.

4 Numerical results and discussions

In this section, we will explore the properties of QSs by solving numerically the differential equations (9)–(11) together with the EoSs (12) and (13), respectively. We then show the impact of model parameters (Σ, β) on the mass–radius relation. Finally, we examine the stability of stellar configurations within this model of gravity via static stability criterion, adiabatic index and checking the sound velocity.

Table 2 The table summarizes results for QS properties, such as the maximum mass $M_{\max}$ and their corresponding radius $R_{\max}$ in units of $M_\odot$ and km, respectively. The range for parameters are $B = 60$ MeV/fm^3 and $\Sigma(x) = 1.1$ with varying $\beta = \in [-1.0, 1.0]$

β	M [$M_\odot$]	R_M [km]	ρ_c [MeV/fm^3]	M/R
-1.0	1.80	11.30	1,294	0.236
-0.5	1.97	11.54	1,238	0.252
0.0	2.15	11.76	1,182	0.270
0.5	2.34	12.03	1,069	0.289
1.0	2.54	12.30	959	0.306

4.1 Profiles for variation of $\Sigma(x)$

More details about the structural properties of QSs have been found in Table 1. Furthermore, it can be seen from Table 1 that the $M_{\max}$ for QS reaches its maximum value of 2.45 $M_\odot$ with radius $R = 12.57$ km for $\Sigma(x) = 1.15$. Furthermore, the results of the maximum mass of QSs are being constraints derived from the available mass and radius measurements of pulsars: PSR J0348+0432 with a mass of $M = 2.01 \pm 0.04 M_\odot$ (LightRed) [64], PSR J0740+6620 with a mass of $M = 2.08 \pm 0.07 M_\odot$ (Pink) [65] and PSR J0952-0607 that corresponds to $M = 2.35 \pm 0.17 M_\odot$ (Magenta) [66] and PSR J1614-2230 with a mass of $M = 2.35 \pm 0.17 M_\odot$ (Purple) [67]. In figure, the shaded areas correspond to the constraints from the binary NS merger GW170817 event [68]. Observing the mass–radius curves from Fig. 1 (upper panel), we can say that our results are comparable with the mass and radius measurements of pulsar observations. More importantly, $\Sigma(x) = 0$ reveals the GR solution with maximum mass greater than 2 $M_\odot$. As a consequence, we see the effect of rainbow function allows us to obtain more massive stars in rainbow gravity. We also investigated the effect of $\Sigma(x)$ on the properties of maximum compactness in the lower panel of Fig. 1. Also in Table 1, we tabulated the value of maximum compactness. Observing the table we see that the value of maximum compactness does not affected for different groups of parameters, and its value is $M/R = 0.3$. We also note that the Buchdahl limit is not violated i.e., $M/R < 4/9$, as shown in Fig. 1.

4.2 Profiles for variation of β

Here we present the outcomes of our numerical analysis for the variation of β. The resulting $(M$–$R)$ and $(M$–$M/R)$ curves are displayed in Fig. 2. We present the results of properties QSs from our calculations in Table 2. Examining the table, we observe that the maximum mass increases with positive increasing values of β, and we find that the maximum mass becomes $M_{\max} = 2.54 M_\odot$ for $\beta = 1.0$. We can also see that the maximum mass exceed the $2M_\odot$ limit when $\beta > 0$ (see Table 2). At the same time we recorded the maximum mass for $\beta = 0$ that represents the isotropic case for

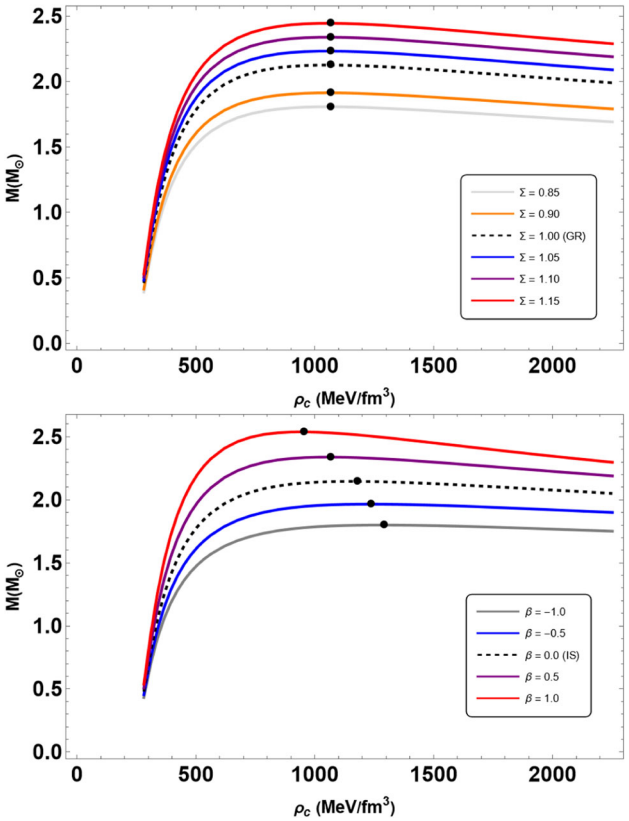

Fig. 3 The M vs ρ_c relations for a family of anisotropic QSs with IQM EoS

QS. It is interesting that the presence of anisotropy leads to higher mass of a star as compared to isotropic case when we vary $\beta > 0$. Moreover, the M–R relations are affected significantly at high mass region due to the presence of an anisotropic pressure. We further impose constraints on the mass–radius relations depending on the measurements of the most massive pulsar observed, as of Fig. 1. Next, we plot the $(M$–$M/R)$ curves in the lower panel of Fig. 2. It is intriguing to note that the parameter β is sensitive to the compactness relation, and the results are tabulated in Table 2 also. From the table we see that by increasing β i.e., when anisotropic effects become stronger, the value of maximum compactness also increases. Here, the Buchdahl limit still meets the con-

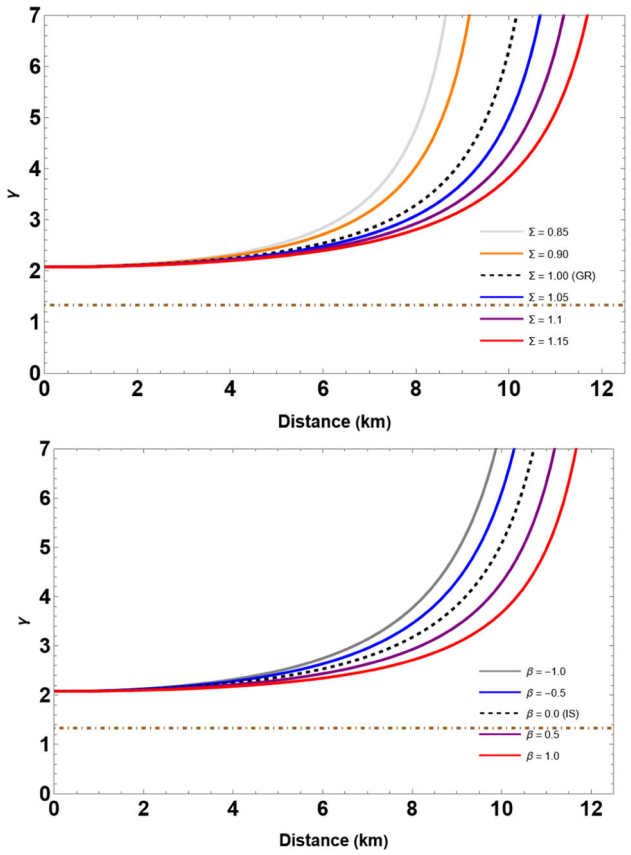

Fig. 4 The adiabatic index as functions of radial coordinate for a family of anisotropic QSs with IQM EoS

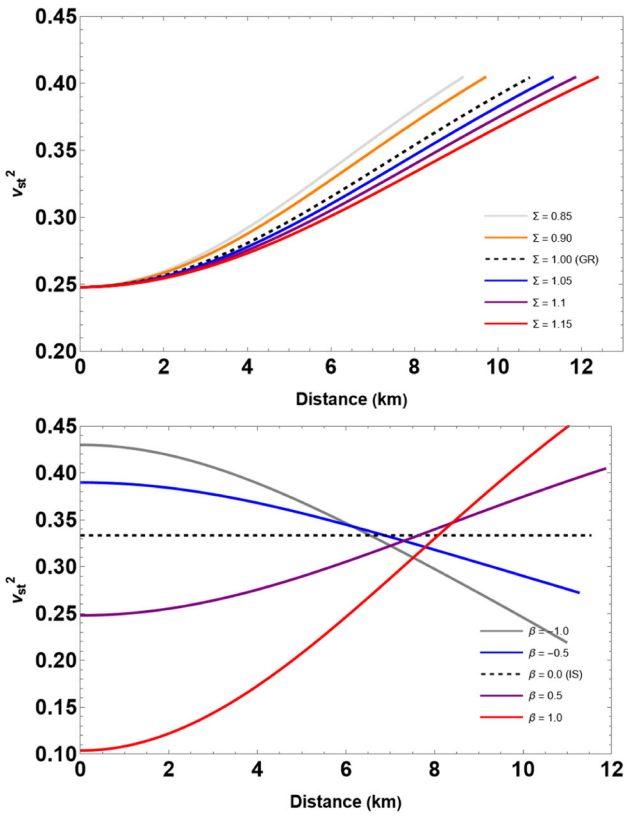

Fig. 5 The squared speed of sound along the tangential direction inside the QSs

straint $M/R < 4/9$, as seen in Fig. 2. Finally, we are tempted to conclude that the presence of anisotropy inside a star leads to more acceptable models than isotropic one.

5 Stability analysis of quark stars

To demonstrate the stability of QSs for anisotropic matter in rainbow gravity, we perform the static stability criterion, adiabatic index and the speed-of-sound. We will discuss all of them step by step with graphical representation.

5.1 Static stability criterion

To address the dynamical stability of an equilibrium solution, we delve deeper into the matter of *static stability criterion* [69,70]. The results are presented in the $M-\rho_c$ plane, where M and ρ_c represent the total mass and central density, respectively. This approach has been widely considered in modified gravity theories, see [71,72] for reviews. We will incorporate this criteria by the following way,

$$\frac{dM}{d\rho_c} < 0 \;\rightarrow \text{indicating an unstable configuration,} \tag{14}$$

$$\frac{dM}{d\rho_c} > 0 \;\rightarrow \text{indicating a stable configuration.} \tag{15}$$

From a conceptual view point, the above criteria represents a necessary condition for stability but not sufficient one. In Fig. 3, we depict the M vs ρ_c curves for the variation of model parameters as of Figs. 1 and 2, respectively. As one can see from figures that transitions from stable to unstable configurations is indicated by the critical points (the black circle), defined by $dM/d\rho_c = 0$. This implies that stable configuration lies in the region where $dM/d\rho_c > 0$.

5.2 Adiabatic indices

Following the above discussion, we next examine the stability of QSs by analyzing the behaviour of the adiabatic index, γ. This idea was developed by Chandrasekhar [73] to study the dynamical stability of an equilibrium configuration, see Ref. [74] for a detail discussion. Since, the adiabatic index γ, governing the perturbations, is expressed as

$$\gamma \equiv \left(1+\frac{\rho}{p}\right)\left(\frac{dp}{d\rho}\right)_S, \tag{16}$$

where the sound speed is define by $dp/d\rho$ is the speed of sound (in units of the speed of light) and the subscript S indi-

cates the derivation at constant entropy. Let us remark that the value of γ is associated with the dynamical instability of relativistic objects has some restrictions for isotropic fluid sphere. The restricted value is known as critical adiabatic index γ_{cr}, and the stability condition leads to the following inequality $< \gamma >> \gamma_{cr}$, where $< \gamma >$ stands for the averaged adiabatic index [75]. In GR context this critical value can be written as $\gamma_{cr} = \frac{4}{3} + \frac{19}{42}C$, where $C = 2M/R$ is the compactness parameter [75]. In the pure Newtonian gravity we always have $\gamma_{cr} = 4/3$, but when the effects of GR make the gravity stronger, γ_{cr} becomes larger than 4/3. In most of the NSs equations of state, its values range from 2 to 4 [76]. On the other hand, authors in [77] have used the Chandrasekhar criterion of stellar instability by employing a large number of realistic EoS of NS matter. Solving the modified TOV equations (9)–(11), we have computed adiabatic index γ in Fig. 4 for several representatives values of $\bar{\lambda}$ and $\Sigma(x)$. The results depicted here indicating a dynamically stable configuration.

5.3 Sound speed and causality

As a last step, we perform the stability of QSs based on checking the speed-of-sound which is determined by the relation $v^2_{r,t} = dp_{\{r,t\}}/d\rho$. Since, we know that the speed of sound should be smaller than the speed of light i.e., $v^2_{r,t} < 1$. Depending on the EoSs (12) and (13), we demonstrate the speed of sound along radial and transverse directions. It should be noted that the radial velocity is constant i.e., $dp_r/d\rho = 1/3$ inside the stellar interior. Whereas the tangential velocity as a function of the radius is displayed Fig. 5 for both cases. The figure shows the standard results of stellar stability still hold in rainbow gravity.

6 Concluding remarks

Advances in nuclear physics and astrophysics have revealed new insights into the internal properties of pulsars that might be strange quark stars (SQS) rather than neutron stars. Because the densities in the core of those objects are exceptionally higher than nuclear saturation density, and supposed to compose of pure quark matter. Aiming this view point, our main object in this article is to study the structural properties of QSs in the framework of rainbow gravity. The basic key ingredient in this formalism is that the geometry of spacetime depends on the energy of the test particle. Here, we investigate the possible method to probe the existence of QS in rainbow gravity.

In this theoretical framework we then present modified TOV equations in spherical symmetry spacetime and solve them numerically to obtain the properties of QSs. In our analysis, we have demonstrated the M–R profiles for anisotropic QSs by varying the model parameters $(\Sigma(x), \beta)$ inside the star. As a result of this choice, the maximum gravitational mass increases with increasing values of $\Sigma(x)$ and β, respectively. We further note that the radius of the star is also increasing with its mass value. Our work demonstrates that the $(M$–$R)$ relations are qualitatively in agreement by the astrophysical constraints on the dense-matter EoS, see Figs. 1 and 2, respectively. In addition, we provide tables for mentioned values of the parameters of our system, such as the maximum masses and their corresponding radii, and the maximum compactness in Table 1 and Table 2, respectively. By examining their behaviour, we can that the maximum compactness is sensitive only on the value of β and the value range changes from 0.236 to 0.306, see 2.

We have also investigated the role of model parameters in the dynamical stability of QS based on the static stability criterion, adiabatic index and checking the sound velocity. Our results clearly show that the standard results of stellar stability, given by both applied methods, still hold in rainbow gravity. Finally, our results suggest that the presence of pressure anisotropy inside a non-rotating star causes a more massive QS with respect to isotropic one. Moving forward, we aim to extend our analysis on this subject in another modified gravity theory in the near future.

Acknowledgements The authors extend their appreciation to the Deanship of Research and Graduate Studies at King Khalid University for funding this work through a Large Research Project under grant number RGP2/453/45. A. Pradhan expresses gratitude to the IUCCA in Pune, India, for offering facilities under associateship programs. B. D. acknowledges support from the administration of University of Nizwa.

Data Availability Statement This manuscript has no associated data. [Author's comment: Data sharing not applicable to this article as no datasets were generated or analysed during the current study.]

Code Availability Statement This manuscript has no associated code/software. [Author's comment: No code/software was generated or analyzed during the production of this manuscript.]

Funded by SCOAP[3].

References

1. G. Baym, T. Hatsuda, T. Kojo, P.D. Powell, Y. Song, T. Takatsuka, Rep. Prog. Phys. **81**, 056902 (2018)
2. M. Feroci et al., LOFT. Exp. Astron. **34**, 415 (2012)
3. E.V. Shuryak, Phys. Rep. **61**, 71 (1980)
4. T. Kojo, AAPPS Bull. **31**, 11 (2021)
5. E.S. Fraga, R.D. Pisarski, J. Schaffner-Bielich, Phys. Rev. D **63**, 121702 (2001)
6. J.C. Jiménez, E.S. Fraga, Phys. Rev. D **102**, 034015 (2020)
7. D.E. Kharzeev, L.D. McLerran, H.J. Warringa, Nucl. Phys. A **803**, 227 (2008)
8. V. Skokov, A.Y. Illarionov, V. Toneev, Int. J. Mod. Phys. A **24**, 5925 (2009)
9. A. Bzdak, V. Skokov, Phys. Lett. B **710**, 171 (2012)
10. D. Grasso, H.R. Rubinstein, Phys. Rep. **348**, 163 (2001)
11. K. Enqvist, P. Olesen, Phys. Lett. B **319**, 178 (1993)
12. S.D.H. Hsu, M. Schwetz, Phys. Lett. B **432**, 203 (1998)
13. E.R. Most, L. Jens Papenfort, V. Dexheimer, M. Hanauske, H. Stoecker, L. Rezzolla, Eur. Phys. J. A **56**, 29 (2020)
14. N. Itoh, Prog. Theor. Phys. **44**, 291 (1970)
15. D.D. Ivanenko, D.F. Kurdgelaidze, Astrophysics **1**, 251 (1965)
16. E. Witten, Phys. Rev. D **30**, 272 (1984)
17. A.R. Bodmer, Phys. Rev. D **4**, 1601 (1971)
18. E. Farhi, R.L. Jaffe, Phys. Rev. D **30**, 2379 (1984)
19. M. Alford, M. Braby, M.W. Paris, S. Reddy, Astrophys. J. **629**, 969 (2005)
20. H. Li, X.L. Luo, H.S. Zong, Phys. Rev. D **82**, 065017 (2010)
21. A.V. Astashenok, S.D. Odintsov, Phys. Rev. D **94**, 063008 (2016)
22. A.V. Astashenok, S. Capozziello, S.D. Odintsov, Phys. Lett. B **742**, 160 (2015)
23. M. Sharif, A. Majid, Int. J. Mod. Phys. A **36**, 2150054 (2021)
24. M. Pace, J.L. Said, Eur. Phys. J. C **77**, 62 (2017)
25. I.G. Salako, M. Khlopov, S. Ray, M.Z. Arouko, P. Saha, U. Debnath, Universe **6**, 167 (2020)
26. E. Gudekli, M.J. Kamran, M. Zubair, I. Ahmed, Chin. J. Phys. **77**, 592 (2022)
27. P. Bhar, K.N. Singh, S.K. Maurya, M. Govender, Phys. Dark Universe **43**, 101391 (2024)
28. R. Saleem, M. Zubair, M.I. Aslam, F. Karamat, Int. J. Geom. Meth. Mod. Phys. **21**, 2450044 (2024)
29. J.M.Z. Pretel, J.D.V. Arbañil, S.B. Duarte, S.E. Jorás, R.R.R. Reis, JCAP **09**, 058 (2022)
30. D. Deb, M. Khlopov, F. Rahaman, S. Ray, B.K. Guha, Eur. Phys. J. C **78**, 465 (2018)
31. J.M.Z. Pretel, T. Tangphati, A. Banerjee, A. Pradhan, Chin. Phys. C **46**(11), 115103 (2022). https://doi.org/10.1088/1674-1137/ac84cb. arXiv:2207.12947 [gr-qc]
32. I.G. Salako, M.J.S. Houndjo, E. Baffou, G.N.R. Amoussou, J. Tossa, Gen. Relativ. Gravit. **54**, 28 (2022)
33. D. Deb, S.V. Ketov, M. Khlopov, S. Ray, JCAP **10**, 070 (2019)
34. Y. Ling, X. Li, H.b. Zhang, Mod. Phys. Lett. A **22**, 2749 (2007)
35. C.Z. Liu, J.Y. Zhu, Gen. Relativ. Gravit. **40**, 1899 (2008)
36. R. Garattini, Phys. Lett. B **685**, 329 (2010)
37. Y. Gim, W. Kim, JCAP **10**, 003 (2014)
38. Z.W. Feng, S.Z. Yang, Phys. Lett. B **772**, 737 (2017)
39. H. Barzegar, M. Bigdeli, G.H. Bordbar, B. Eslam Panah, Eur. Phys. J. C **83**, 151 (2023)
40. R. Garattini, EPJ Web Conf. **58**, 01007 (2013)
41. A.B. Tudeshki, G.H. Bordbar, B. Eslam Panah, Phys. Lett. B **835**, 137523 (2022)
42. S.H. Hendi, G.H. Bordbar, B.E. Panah, S. Panahiyan, JCAP **09**, 013 (2016)
43. G. Amelino-Camelia, Int. J. Mod. Phys. D **11**, 35 (2002)
44. J. Kowalski-Glikman, arXiv:gr-qc/0603022 [gr-qc]
45. J. Magueijo, L. Smolin, Class. Quantum Gravity **21**, 1725 (2004)
46. B.P. Abbott et al. [LIGO Scientific and Virgo], Phys. Rev. Lett. **116**, 061102 (2016)
47. B.P. Abbott et al. [LIGO Scientific and Virgo], Phys. Rev. X **9**, 031040 (2019)
48. R. Abbott et al. [LIGO Scientific and VIRGO], Phys. Rev. D **109**, 022001 (2024)
49. A. Chodos, R.L. Jaffe, K. Johnson, C.B. Thorn, V.F. Weisskopf, Phys. Rev. D **9**, 3471 (1974)
50. G. Fiorella Burgio, A.F. Fantina, Astrophys. Space Sci. Libr. **457**, 255 (2018)
51. D. Blaschke, N. Chamel, Astrophys. Space Sci. Libr. **457**, 337 (2018)
52. F. Sandin, Eur. Phys. J. C **40**, 15 (2005)
53. S. Joshi, S. Sau, S. Sanyal, JHEAp **30**, 16 (2021)
54. J.D.V. Arbañil, G.A. Carvalho, R.V. Lobato, R.M. Marinho, M. Malheiro, Phys. Rev. D **100**, 024035 (2019)
55. D. Horvat, S. Ilijic, A. Marunovic, Class. Quantum Gravity **28**, 025009 (2011)
56. D.D. Doneva, S.S. Yazadjiev, Phys. Rev. D **85**, 124023 (2012)
57. H.O. Silva, C.F.B. Macedo, E. Berti, L.C.B. Crispino, Class. Quantum Gravity **32**, 145008 (2015)
58. K. Yagi, N. Yunes, Phys. Rev. D **91**, 123008 (2015)
59. J.M.Z. Pretel, Eur. Phys. J. C **80**, 726 (2020)
60. A. Rahmansyah, A. Sulaksono, A.B. Wahidin, A.M. Setiawan, Eur. Phys. J. C **80**, 769 (2020)
61. A. Rahmansyah, A. Sulaksono, Phys. Rev. C **104**, 065805 (2021)
62. V. Folomeev, Phys. Rev. D **97**, 124009 (2018)
63. L. Herrera, W. Barreto, Phys. Rev. D **88**, 084022 (2013)
64. J. Antoniadis, P.C.C. Freire, N. Wex et al., Science **340**, 6131 (2013)
65. E. Fonseca, H.T. Cromartie, T.T. Pennucci et al., Astrophys. J. Lett. **915**, L12 (2021)
66. R.W. Romani, D. Kandel, A.V. Filippenko et al., Astrophys. J. Lett. **934**, L17 (2022)
67. E. Fonseca, T.T. Pennucci, J.A. Ellis et al., Astrophys. J. **832**, 167 (2016)
68. B.P. Abbott et al. [LIGO Scientific and Virgo], Phys. Rev. Lett. **121**, 161101 (2018)
69. B.K. Harrison, *Gravitational Theory and Gravitational Collapse* (University of Chicago Press, Chicago, 1965)
70. Y.B. Zeldovich, I.D. Novikov, *Relativistic Astrophysics, Vol. I: Stars and Relativity* (University of Chicago Press, Chicago, 1971)
71. H. Maulana, A. Sulaksono, Phys. Rev. D **100**, 124014 (2019)
72. Y.H. Sham, L.M. Lin, P.T. Leung, Phys. Rev. D **86**, 064015 (2012)
73. S. Chandrasekhar, Astrophys. J. **140**, 417 (1964)
74. E.N. Glass, A. Harpaz, Mon. Not. R. Astron. Soc. **202**, 1 (1983)
75. C.C. Moustakidis, Gen. Relativ. Gravit. **49**, 68 (2017)
76. P. Haensel, A.Y. Potekhin, D.G. Yakovlev, Astrophys. Space Sci. Libr. **326** (2007)
77. P.S. Koliogiannis, C.C. Moustakidis, Astrophys. Space Sci. **364**, 52 (2019)